Title: Subsurface robotic exploration for geomorphology, astrobiology, and mining during MINAR6 campaign, Boulby Mine, UK: Part II (Results and Discussion)

Short Title: Subsurface robotic exploration during MINAR6 campaign

Authors: Thasshwin Mathanlal[1*], Anshuman Bhardwaj[2], Abhilash Vakkada Ramachandran[1], María-Paz Zorzano[4,2,1], Javier Martín-Torres[1,2,5] and Charles S. Cockell[6]

[1] Atmospheric Science, Department of Computer Science, Electrical and Space Engineering, Luleå University of Technology, Luleå 97 187 Sweden; E-mail: thasshwin.mathanlal@ltu.se; Telephone: +46722166779

[2] School of Geosciences, University of Aberdeen, Meston Building, King's College, Aberdeen, AB24 3UE, UK

[3] National Space Science and Technology Center, United Arab Emirates University, P.O. Box 15551, Al Ain, Abu Dhabi, UAE

[4] Centro de Astrobiología (CSIC-INTA), Torrejon de Ardoz, 28850 Madrid, Spain; E-mail: maria-paz.zorzano.mier@ltu.se

[5] Instituto Andaluz de Ciencias de la Tierra (CSIC-UGR), 18100 Granada, Spain; E-mail: javier.martin-torres@ltu.se

[6] UK Centre of Astrobiology, SUPA, School of Physics and Astronomy, University of Edinburgh, Edinburgh, Midlothian, United Kingdom; E-mail: c.s.cockell@ed.ac.uk

* Corresponding Author (thasshwin.mathanlal@ltu.se)

ABSTRACT

Geomorphological studies of the hidden and protected subsurface environments are crucial to obtain a greater insight to the evolution of planetary landforms, hydrology, climate, geology, and mineralogy. From an astrobiological point of view subsurface environments are of interest for their potential habitability as they are local environments that are partially or fully shielded from the high levels of space and solar radiation. Furthermore, in the case of Mars, there is an increasing interest in searching for the presence of past or extant life in its subsurface. These applications make it mandatory to investigate equipment and instrumentation that allow for the study of subsurface geomorphology, as well as organic chemical biomarkers, such as biomolecules, carbon, nitrogen and sulphur isotopes, and other biologically significant minerals and gases. Mines on Earth can be used as analogues to investigate the geomorphology of Martian subsurface environments and perform astrobiology studies. With that goal, we have developed a low-cost, robust, remotely operable subsurface rover called KORE (KOmpact Rover for Exploration). This work illustrates the studies of a terrestrial analogue for the exploration of Mars using KORE during the Mine Analogue Research 6 (MINAR 6) campaign with the low-cost 3D mapping technology InXSpace 3D (In situ 3D mapping tool eXploration of space 3D). InXSpace 3D utilizes a RGB-D camera that captures depth information in addition to the RGB data of an image, operating based on the structured light principle capable of providing a depth information in mm scale resolution at sub 3m mapping range. InXSpace 3D is used to capture point clouds of natural and artificial features, thereby obtaining information about geologically relevant structures and also to incorporate them in earth mining safety. We tested two of the dense Simultaneous Localization and Mapping (SLAM) algorithms: Kintinuous and Real-Time Appearance-Based Mapping (RTAB-Map) to check the performance of InXSpace 3D in a dark mine environment. Also, the air accumulation of

volatiles such as methane and formaldehyde due to thermogenic and mining process was measured with the environmental station payload on the rover platform, which caters to both astrobiological significance and mine safety. The main conclusions of this work are: (1) a comparison made between the RTAB-Map algorithm and Kintinuous algorithm showed the superiority of Kintinuous algorithm in providing better 3D reconstruction; although RTAB-Map algorithm captured more points than the Kintinuous algorithm in the dark mine environment; (2) a comparison of point cloud images captured with and without lighting conditions had negligible effect on the surface density of the point clouds; (3) close-range imaging of the polygonal features occurring on the halite walls using InXSpace 3D provided mm-scale resolution to enable further characterisation; (4) heuristic algorithms to quickly post-process the 3D point cloud data provided encouraging results for preliminary analyses; (5) we successfully demonstrated the application of KORE to mine safety; and (6) the multi-sensors platform on KORE successfully monitored the accumulated volatiles in the mine atmosphere during its operation. The findings obtained during this KORE campaign could be incorporated in designing and planning future subsurface rover explorations to potential planetary bodies such as Mars with synergistic applications to subsurface environments in mines on Earth.

Keywords: Rover development, 3d-mapping, geomorphology, astrobiology, mining, COTS.

Introduction

Subsurface environments of a planetary body have their own geomorphological and astrobiological significance as they are partially or fully shielded from the atmosphere and radiations (Dartnell et al., 2007). In particular, in the case of Mars, caves have been proposed as Special Regions which require planetary protection measurements because of their potential to sustain terrestrial life. They also are of interest as shelter for the future human exploration of

Mars (Rummel et al., 2014; Martín-Torres et al., 2020). Subsurface environments influence the surface environment directly and indirectly. For example, on Earth, subsurface ground aquifers contribute to the Earth's hydrology and the interaction with the surface is one of the main processes of water exchange in the planet. Subsurface aquifers have also been reported to support plate tectonics (Oliver, 1986, Bethke, 1990) on Earth. Moreover, there is a diverse microbial ecology in the extreme subsurface environments on Earth, highlighting the astrobiological importance of such studies (Wang, Xue and Ma, 2010).

Until the commissioning of the Mars Advanced Radar for Subsurface and Ionosphere Sounding (MARSIS) instrument aboard the ESA Mars Express mission (Giovanni et al., 2005), there was no direct observation of the unexposed Martian crust except for the study of exposed features such as crater and valley walls through high resolution photography obtained through the Mars Orbiter Camera (Malin and Edgett, 2001) and the High Resolution Imaging Experiment (HiRISE) onboard the Mars Reconnaissance Orbiter (MRO) (Grant et al., 2008). Since the Mariner 9 mission to Mars, outflow channels have been detected in the Elysium region of Mars, indicating the presence of subsurface volatile reservoirs (Christiansen, 1985). The recent Martian breakthrough discoveries such as the detection of putative sub-glacial liquid water below the ice in the south pole layer deposits (Orosei et al., 2018), the detection of methane plumes within the Gale crater (Webster et al., 2014), exposed ice sheets in the mid-latitudes (Dundas et al., 2018) and seasonal variation of the atmospheric composition along Gale crater (Trainer et al., 2019) have further raised interest in exploring the subsurface of Mars and potentially habitable environments where there is an interaction with the surface environments. Geomorphological studies of subsurface environments are crucial to obtain a greater insight to the evolution of planetary landforms, hydrology, climate, geology, and mineralogy. The uniqueness of the Martian subsurface environments for geomorphological studies have been

117 elucidated by Dundas et al. (2018), where radar soundings indicate the presence of debris-
118 covered glaciers (Holt et al., 2008, Plaut et al., 2009) as well as buried regional ice sheets. The
119 volcanic, tectonic and hydrological history of the extraterrestrial bodies can also be obtained
120 from the study of subsurface environments. Monitoring subglacial environments (e.g., Jacob et
121 al., 2011) has shown evidence of climate change impacting the glacial systems. Also, the study
122 of subsurface geology with its implication for the survival of biosignatures has been discussed
123 by Dartnell et al. (2007). With the state of the art exploration focussed on the study of organic
124 chemical biomarkers, carbon and sulphur isotopes, biologically significant minerals to search
125 for the presence of past or extant life on Mars, the new approach to biosignature detection
126 involves study of biogeomorphological characteristics (Gorbushina et al., 2004; Naylor, 2005;
127 Cady and Noffke, 2009; Noffke et al., 2013; Westall et al., 2015). This approach to explore
128 Martian astrobiology through geomorphological analysis of surface and subsurface features on
129 earth analogues has been reported by Corenblit et al. (2019).
130
131 The understanding of the evolution of ancient climate and the development of life on Earth has
132 been derived from the study of mineralogical, textural, and geochemical signatures preserved
133 in the sedimentary rock record in stratigraphic sections (De Sanctis et al., 2017). Surface
134 environments of Mars are rich in sedimentary outcrops that exhibit visible stratigraphic features
135 at a range of spatial scales (e.g., Malin and Edgett, 2000, 2003; Grotzinger et al., 2006; Dromart
136 et al., 2007; Lewis et al., 2008; Milliken et al., 2010), thus highlighting the importance of
137 studying subsurface layering and compositions.
138
139 We have developed a subsurface operable rover called KORE (KOmpact Rover for
140 Exploration) to facilitate the autonomous investigation of the geomorphology of subsurface
141 environments and perform astrobiology studies in Martian analogues, with applications to

mining on earth. KORE has been designed making use of commercial off the shelf components (COTS). KORE is a large, semi-autonomous rover weighing 160 kg with L x W x H dimensions 1.2 m x 0.8 m x 1 m and a payload carrying capacity of 100 kg using 800 W traction power that can power to a maximum speed of 8.4 km/hr. The design and development of the rover for analogue research in mines on Earth has been elucidated in Mathanlal et al. (2019). This manuscript is a continuation of that work where a nominal operation of the rover is demonstrated. It demonstrates the use the low-cost, robust, and remotely operable subsurface rover KORE to perform geomorphology, astrobiology and environmental characterization studies during its operation in the Mine Analog Research (MINAR6) campaign during September 2018 in the Boulby mine (UK).

MINAR6 campaign

MINAR is an advanced series of subsurface exploratory research to study the mine environments as a Mars analogue for geological, geomorphological, and astrobiological research, building on potential collaboration between planetary scientists within an active mine. The MINAR programmes enhance the testing and development of instruments and scientific studies related to the robotic and human exploration of the deep subsurface (Bowler 2013; Payler et al., 2016; Cockell et al., 2018). One of the main identified research gaps in this direction was demonstrating synergy between space technology and mining. Though space and mining represent two potentially separate facets of technology, there is a great scope for incorporating technology used in these fields in a synergistic manner. The comprehensive nature of the MINAR campaigns provide an ideal scenario to test new scientific instruments and technologies and also gather useful and reliable data for meeting the needs of research in deep subsurface environments. The MINAR6 campaign was a more concise version,

succeeding the MINAR5 campaign with a focus on subsurface robotic exploration. The two-week campaign was a hypothesis driven campaign, and in this work, we summarize the results related to some of these hypotheses. One of the hypotheses was that the autonomous monitoring of the distances and shapes of certain natural or artificial features could be performed using a low-cost, robust 3D mapping point cloud generation system that can be used to: 1) inform about geologically relevant structures; and 2) inform about safety of the mine. The second hypothesis is that in an enclosed subsurface environment, the air may be accumulating volatiles. Some of them are potentially hazardous to the miners and monitoring them remotely is necessitated. The second hypothesis though deviates from the domain of astrobiology, is a crucial synergistic application of an astrobiological exploration tool for human safety which not only caters to terrestrial mining but also to future human space exploration of extra-terrestrial subsurface or enclosed environments on the Moon or Mars. A corroboration between astrobiology exploration with human safety is elucidated in (Lim et al., 2019) where the design of NASA Biologic Analog Science Associated with Lava Terrains (BASALT) research program is discussed. Finally, autonomous robotic exploration is always the first step in space exploration and monitoring, in a cave environment, the accumulation and release of volatiles may also be important to understand other surficial processes like methane or oxygen release which have been observed robotically on the surface of Mars by the Curiosity rover (Webster et al., 2018, Trainer et al., 2019) and may have their origin in the subsurface. To validate these hypotheses, the KORE rover platform was updated with a set of low-cost dedicated instruments. The instruments aboard the rover provided useful and reliable data for meeting the research needs which are highlighted in this paper. Logistics issues and active mining work restricted the accessible region close to the Boulby Underground Laboratory. Though with the limited operating spatial area, most of the requirements to validate the hypothesis were justified.

Materials and Methods

KORE is a low cost, robust rover platform designed to carry a wide suite of instruments for subsurface exploration in extraterrestrial analogue environments and key terrestrial environments such as mines. KORE is built with a robust design maximizing the use of COTS components and minimum custom-made parts to facilitate intelligibility to the research community to build such robotic platforms with a conservative budget without compromising the quality. The design ensures quick construction of the rover and improves portability of the rover to different field sites. The components used in the development of KORE are easily accessible and improve the serviceability of the rover in case of any failure. Moreover, the rover has the provision for easy and instant integration of more sensors as per the user requirements (Mathanlal et al., 2019). The In-situ 3D mapping tool eXploration of space 3D (InXSpace 3D) system, LASER-based methane detector and environmental sensors are the most critical instruments aboard the KORE rover. Figure 1 shows KORE during operation in the MINAR 6 campaign with the major components marked in the image.

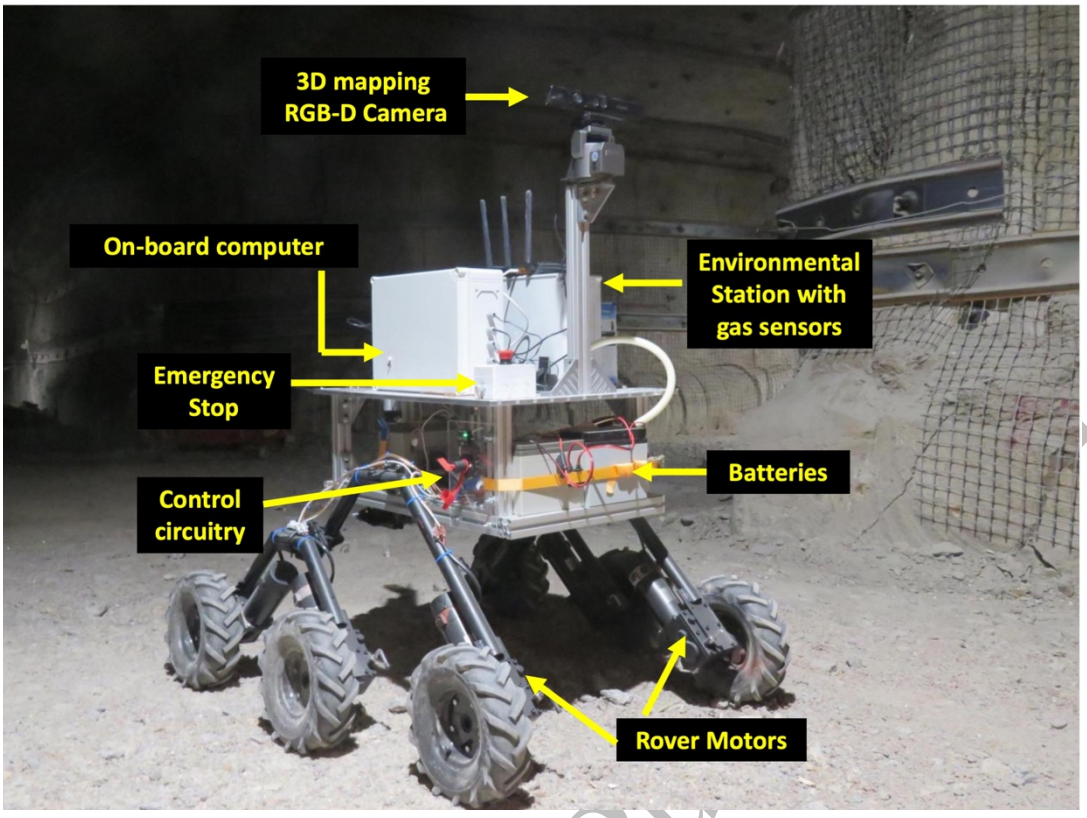

Fig. 1. KORE rover operating in the Boulby mine during MINAR 6 campaign. The equipment is marked.

InXSpace 3D system

The InXSpace 3D system is a real time 3D mapping system designed using a Microsoft Kinect™ first generation camera that works based on Structured Light technology where the camera projects an active pattern and obtains the depth information by analysing the deformation of the pattern. The Microsoft Kinect™ camera also has a depth error in the order ≤ 1 mm to 75 mm depending upon the measurement distance from the sensor. Below 3 m the error rate is less than 1 mm, which justifies its application to short range mapping. The total mapping range of the Kinect camera is 0.8 m to 4 m.

LASER-based methane detector

The KORE rover utilizes a portable drone-mounted remote laser methane detection system from Hesai photonics. The methane detector works based on absorption spectroscopy and is pre-calibrated in the factory and is operable in the field out of the box. However, the methane detector was tested, and the readings were validated, in laboratory conditions before mounting on the KORE rover. The detector provides a methane concentration output which is the integrated concentration of methane along the path of the laser beam. The specifications of the methane detector can be found in Table 5 of the first paper (Mathanlal et al., 2019).

Environmental Station

The Environmental Station on the KORE Rover has a multitude of sensors measuring common air pollutants, particulate matter and environmental parameters such as temperature, pressure and relative humidity. The gases measured are NO_2, SO_2, H_2S, formaldehyde, CO, CO_2, O_3, O_2, and volatile organic compounds (VOC). Ultra-Low Power Analog Gas Sensor Modules (ULPSM) from Spec Sensors are used to measure the gases NO_2, SO_2, H_2S, CO, O_3 and VOC. Formaldehyde measurements are obtained from DFRobot Air Quality Monitor module. O_2 measurement is obtained using digital UV Flux 25% Oxygen Sensor from CO2meter and CO_2 measurement is obtained from The CozIR®-A 2,000 ppm CO2 Sensor from CO2meter. These sensors are pre-calibrated in the factory and have been particularly chosen for its pre-calibration which dissuades the need to perform a calibration procedure before deployment, saving cost and time. An Arduino microcontroller is employed in the retrieval of these gases and the data is stored onboard the environmental station computer. The data can be accessed through the rover computer or also directly from the environmental station itself. The environmental station provides a vivid characteristic of the environment around the rover.

During the MINAR6 campaign, a number of experiments were performed with these instruments onboard with a 6-day experimentation window with a total experimentation time of ~22 hours. MATLAB and Cloud Compare software were extensively used during the analysis of the experiments.

Results and Discussion

Algorithm testing with InXSpace 3D

During the MINAR6 campaign, experiments were made with two dense Simultaneous Localization and Mapping (SLAM) algorithms, Kintinuous (Whelan et al., 2012) and Real-Time Appearance-Based Mapping (RTAB-Map) (Labbé and Michaud, 2018), to choose the best algorithm for InXSpace 3D system. These two dense SLAM algorithms were chosen for study as they were compatible with the OpenNI driver through which the Microsoft Kinect first generation camera was interfaced to the onboard Nvidia JETSON computer. The region along the mine shaft walls were chosen to test the resolution of the system with its capability to generate a point cloud with very minute details. The features along the mine shaft walls with the ground provided an ideal scenario to validate the 3D reconstruction capabilities of the algorithms used. KORE was made to perform two traverses with each algorithm loaded on a traverse. The traverses were made with identical velocity to ensure that both the algorithms had the similar time for scanning. The results from the two algorithms are shown in Figure 2. It could be determined from the reconstructed Digital Terrain Model (DTM), that the Kintinuous algorithm produced a more pronounced point cloud compared to the RTAB-Map. The RTAB-Map captured more points than the Kintinuous algorithm but suffers from poorer reconstruction of 3D map from the points. Figure 3 shows the histogram plot that indicates the number of

points captured by each of the algorithms against the co-ordinate distance along z-axis. The spectral color coding in the histogram marks the depth information of the points along the z-axis, with blue indicating points close to the ground and red in the farthest vertical height from the ground, as seen in the Figure 2. As clear from Figure 3, RTAB-Map captured a larger portion of the wall in the same lighting conditions from the fixed point of observation, resulting in a greater number of points (Figure 3). However, the point density of Kintinuous (7637 points/m^2) was better and that resulted in an extremely well-constructed DTM where even cm-scale pebbles on the surface or minor grooves in the mine wall were clearly discernible. Thus, the use of either of these algorithms can be attributed to the user need for either higher resolution DTM or covering larger area in lesser time at coarser resolutions.

284

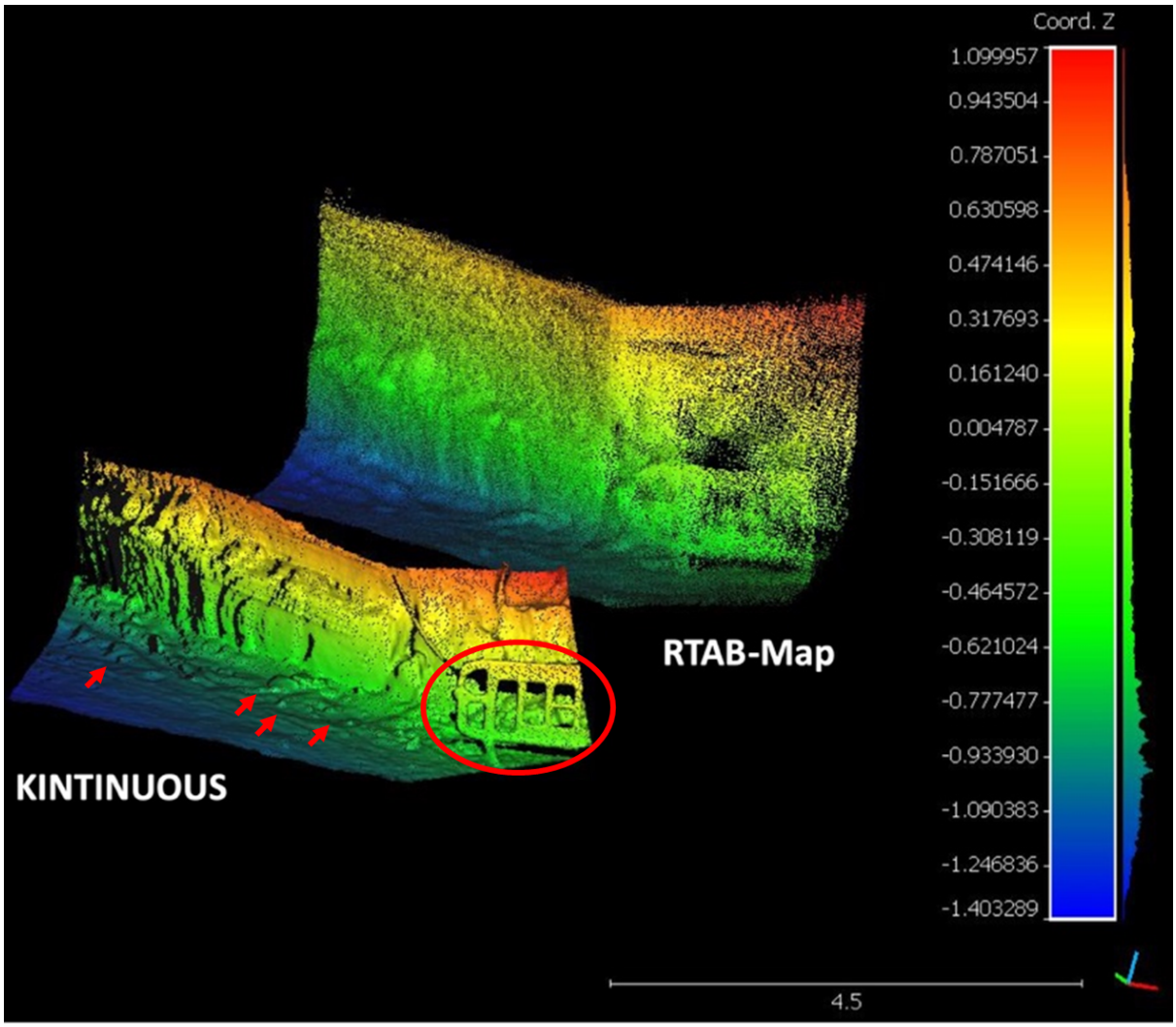

285

286 **Fig. 2.** Digital Terrain Model (DTM) of mine shaft walls generated from point cloud obtained
287 through two different dense SLAM algorithms – Kintinuous and RTAB-Map. The scale bar is
288 in m. The red ellipse marks the barricade that was not resolved by RTAB-Map and the red
289 arrows mark the pebbles and rocks on the surface.

290

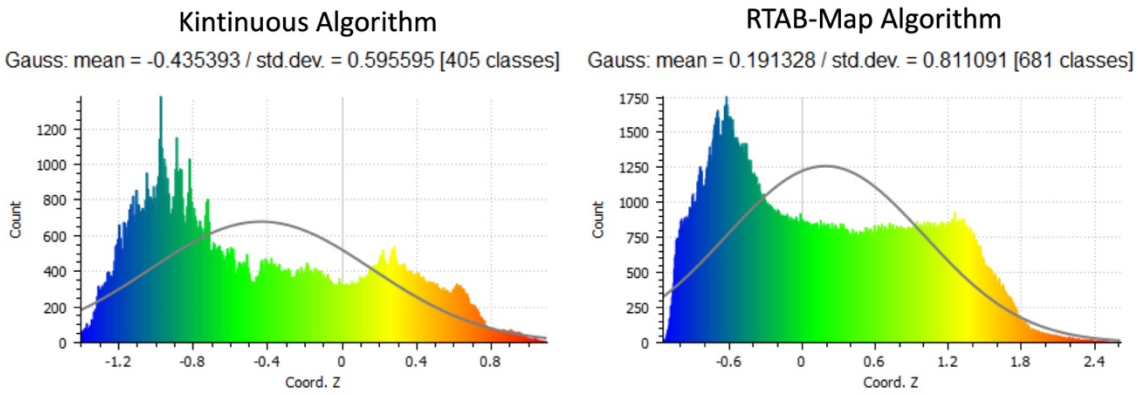

Fig. 3. Histogram of the points in the point cloud image along the z-direction for both the algorithms – Kintinuous (left) and RTAB-Map (right). The scaling in both the algorithms is different accounting for the observed differences in z-coordinates.

A detailed comparison between Kintinuous and RTAB-Map algorithm is elucidated by (Altuntas et al., 2017). Both the algorithms are visual SLAM systems but however their approach to map features result in different performance rates. Kintinuous is more dependent on depth data, while RTAB-Map effectively uses RGB data. Since, lighting conditions in subsurface environments are limited, the RTAB-Map suffers poor reconstruction of point cloud giving Kintinuous an upper hand in 3D reconstruction of the point clouds. Thus, the further analyses of InXSpace 3D performance in this paper has been evaluated using Kintinuous algorithm as we were more interested in observing the clarity of reconstructed 3D terrain. InXSpace 3D can operate in pitch black dark scenarios owing to the presence of the infrared projector and scanner. The Microsoft Kinect camera projects a structured infrared light against the target to determine the depth information, which is then combined with the RGB-data. The Kintinuous algorithm uses these two data sets to obtain the 3D point cloud, enabling the capability to operate under varied lighting conditions. However, the influence of lighting on the point cloud generation with the Kintinuous algorithm was tested to determine if there was any significant drop in efficiency with zero lighting conditions. KORE was made to perform two traverses at identical velocities with onboard lights switched on and switched off. The

DTMs obtained from the point clouds generated by Kintinuous algorithm during the two traverses are shown in Figure 4.

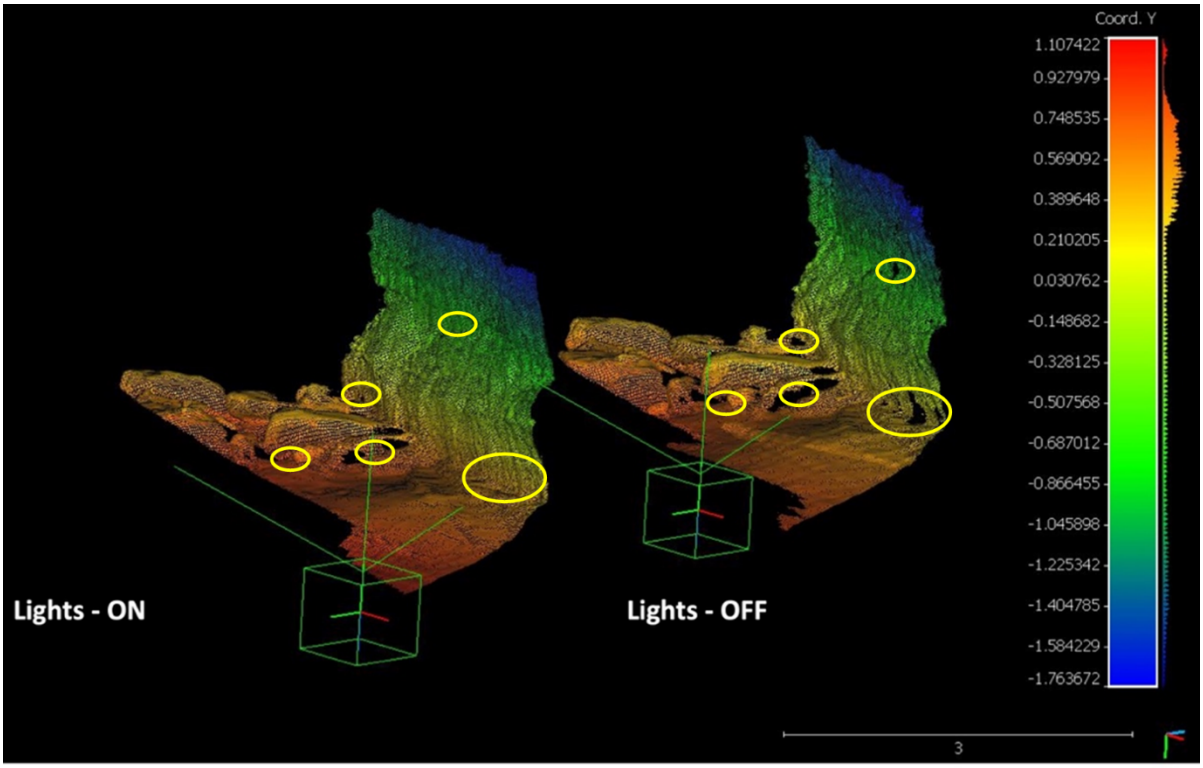

Fig. 4. DTM obtained from the point cloud captured using Kintinuous algorithm in two conditions - Lights ON and Lights OFF. The green box denotes the camera position and orientation at the beginning of the scan. The scale bar is in m. The yellow ellipses highlight the blank regions in Lights-OFF conditions.

It could be seen from both the DTMs of the mine shaft walls that the point clouds are remarkably similar except for a few blanks (yellow ellipses in Figure 4) in the lights-off condition. The reason for the loss of points in the lights-off condition is attributed to the operation of the Kintinuous algorithm. The Kintinuous algorithm uses two methods to estimate the pose, with geometric estimation being the first method utilized. This method matches the infrared depth data with the closest point in the scanned 3D volume. The second method utilizes the photometric estimation by comparing RGB data from two consecutive frames. The Kintinuous algorithm then estimates the final pose by taking a weighted sum of the geometric and photometric estimation. As elucidated in (Altuntas et al., 2017), Kintinuous primarily uses

depth data than RGB-data for the 3D reconstruction of point clouds. With the presence of lights in the later scenario, the availability of more RGB data points provides a slightly better pose estimation of the point clouds. A statistical evaluation of the surface density of the point clouds under both lights-on and lights-off condition is shown in the Figure 5.

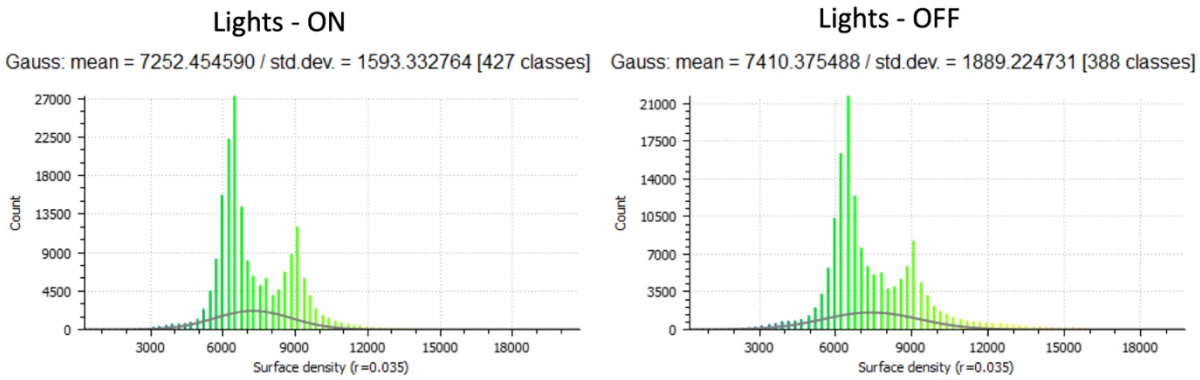

Fig. 5. Surface density of the point clouds under lights on condition (left) vs the surface density of the point clouds under lights off condition (right). The Kernel size of the points in both cases is 0.035.

The graph on the left shows denser point cloud counts observed in the lights-on condition, whereas, the graph on the right shows a rarer point cloud counts in the lights-off condition. This explains the few blank spots observed in the DTM image of the mine shaft walls. However it could be determined that the surface density profile of the point clouds were very similar. This shows that the resolution obtained in both the cases is indistinguishable. Thus it is validated that the InXSpace 3D system has a very good capability of 3D reconstruction in pitch black conditions.

Mapping of polygonal features with InXSpace 3D

One of the most interesting geomorphological features found in the Boulby mine are the dark lined polygon features observable in the ceiling of the mine shafts which represents a 250

352 million-year-old Permian evaporitic deposit. Figure 6 shows the RGB image of the polygon
353 feature observed in the Boulby mine.

354

355 **Fig. 6.** RGB-image of the polygons observed in the mine shaft of the Boulby mine.

356

357 These polygons with black rims and white salty matrix in the middle are hypothesized to be
358 remnant minerals from the Zechstein that generated these evaporitic deposits 250 million years
359 ago. During the MINAR 5 campaign (Cockell et al., 2018), samples were taken by sterile
360 drilling of cores and the samples were analysed for the presence of lipid biomarkers. The recent
361 analysis of the lipid biomarker has revealed the presence of very low abundance of biomass
362 dominated by primarily alkanes and low levels of hopanes and steranes which are proposed to
363 have been uniformly distributed along the interior of the polygons quite rapidly before the
364 crystallization of the halite (Wilhelm et al., 2019). The study also concludes that lipid
365 biomarkers should have been from a terrestrial source and they have not undergone a significant
366 thermal maturation since their deposition. The formation mechanisms of the polygons are not
367 precisely known. They could be desiccation cracks, cracks caused by thermal contraction or

368 they could be formed by other mechanisms (e.g. Warren, 1999; Abbott, 2016). In the case of
369 desiccation, tepee-like structures are often formed (Warren, 1999). The black rimmed polygons
370 which were studied for lipid biomarkers were scanned with InXSpace 3D system to look for
371 any observable tepee projections along the black rim of the polygons. Figure 7, shows the 3D
372 point cloud image of the polygon feature (left) and the DTM of the corresponding 3D point
373 cloud image. The InXSpace 3D was positioned such that the Kinect camera was pointing
374 straight up to the polygons (Z-axis) on the ceiling, parallel to the polygon plane.

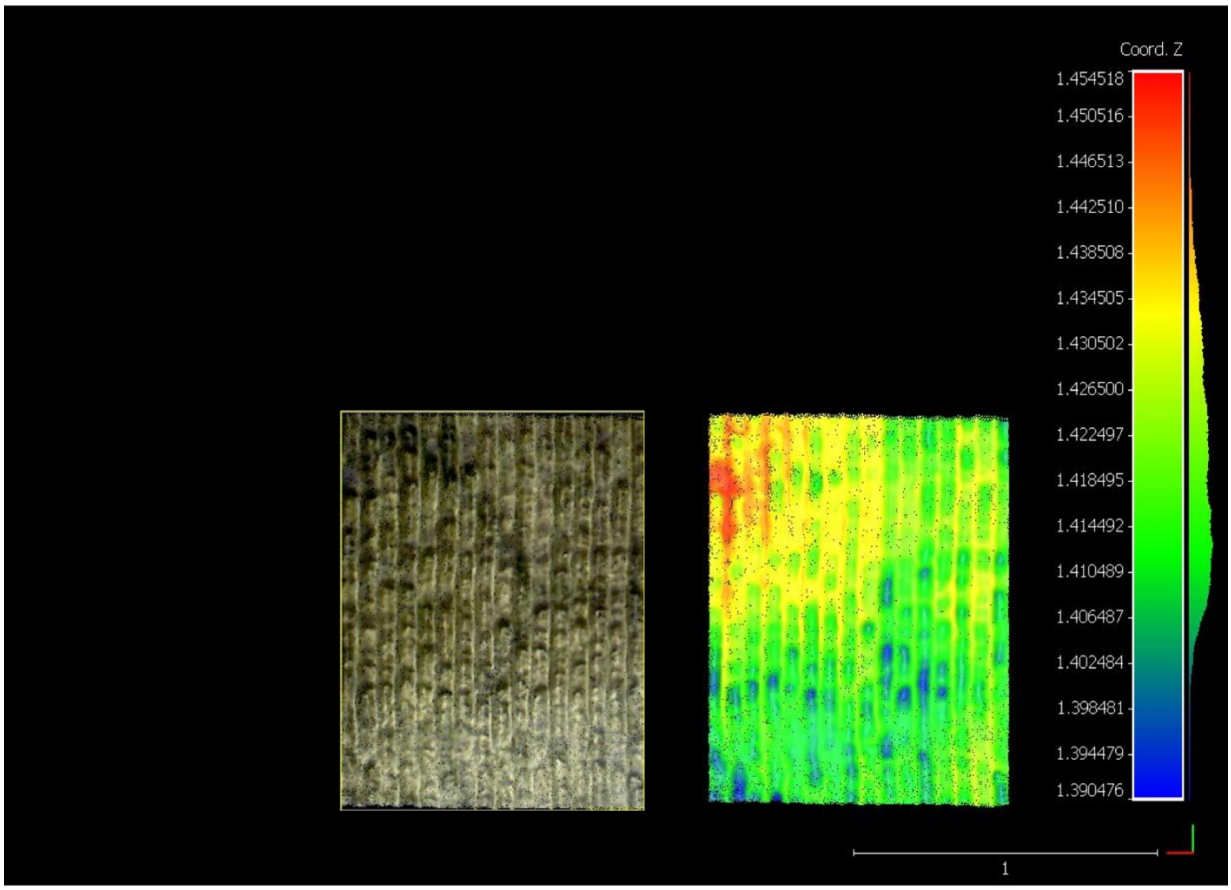

375

376 **Fig. 7.** (left) RGB point cloud of the polygon; (right) DTM analysis of the polygon feature. The
377 camera was positioned along the z-axis parallel to the polygon plane. The scale bar is denoted
378 in m.

379

380 From the DTM it could be found that there is no tepee pattern observable corresponding to the
381 black rims of the polygon. This case shows however the ability to observe 3D features with a
382 very high resolution of 4 mm, which in this case are artificial and have been produced by the

tools that were used to scrape this wall and expose the polygons. This was a case-specific scenario where the topographic changes were not present in the underlying polygon and only colour differences were marking the polygon boundaries. Thus, it does not mean that the system is unable to detect the topographic changes if they are actually present in another scenario or the algorithm is unable to make use of such detected topographical information in mapping. In spite of the absence of 3D features, the observable colour variations could indicate the presence of a different product, accumulated through a contraction-expansion process and/or a water cycle process. This boundary may concentrate different minerals, and create a different environment where biomarkers may have been preserved. These data show the potential for the use of this type of imaging for geomorphological analysis on Earth and in the subsurface of extraterrestrial bodies. Geomorphological mapping system cannot be considered as an absolute tool to study biomarkers but it is of course an accessory, as demonstrated by InXSpace 3D, that may be used for sample selection. The evolution of life on Earth has led to the formation of several biogeomorphological changes in the landforms and surface processes (Viles, 1988; Butler, 1995). Extending the capability of the InXSpace 3D apart from RGB imaging and depth map generation, an image processing framework has been developed in MATLAB to characterize the corner points in the polygon features. The framework was originally built to analyse polygons on Mars through the HiRISE images obtained from the Mars Reconnaissance Orbiter (MRO). Figure 8, shows the HiRISE image of the Martian polygon dunes, captured by the MRO on 18th March 2013.

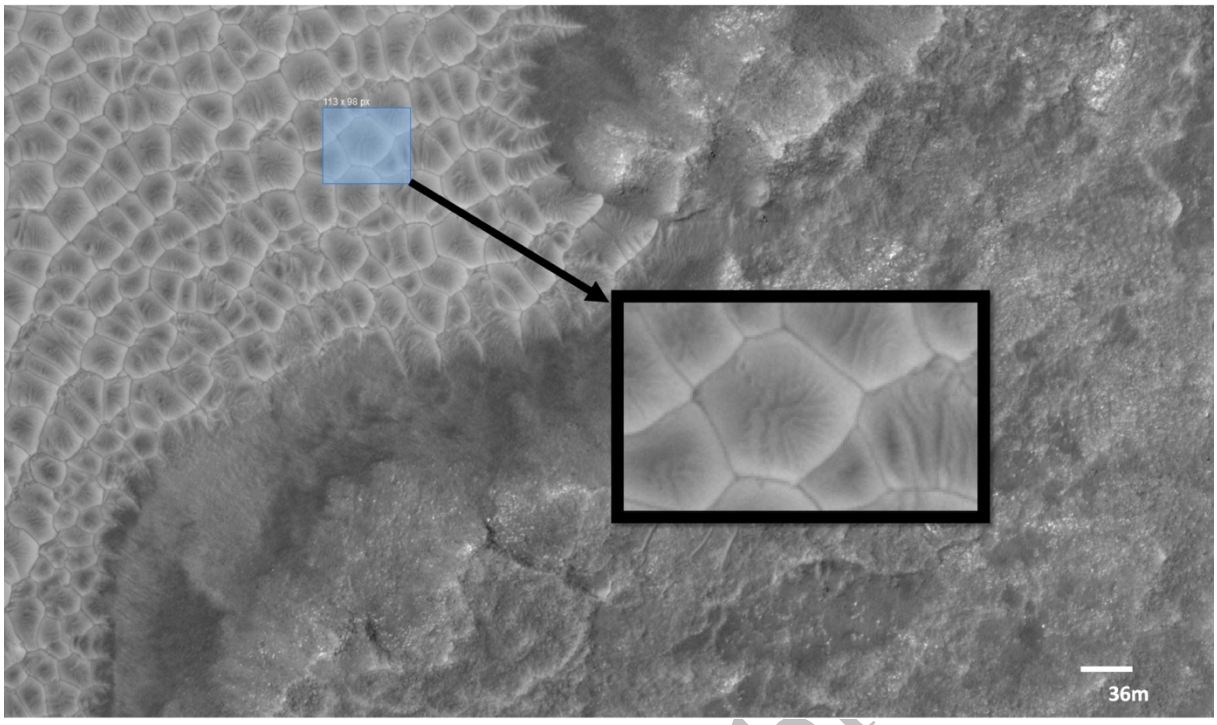

Fig. 8. HiRISE image of polygonal dunes of Mars (ESP_031138_1380) in original size (scale factor 1) with the inset image showing a zoomed-in polygonal dune (scale factor 10).

The reason for the formation of such polygonal geomorphological shapes on Mars often vary with many mechanisms put forth such as aeolian processes, thermal contraction, desiccation, volcanic, and tectonic processes (Mutch et al., 1976, 1977; Lucchita, 1983; Pechmann, 1980; Seibert and Kargel, 2001; Mangold, 2005). Figure 9, shows the sequence of operations performed by the image processing framework to obtain the information regarding the dimensions of a scanned polygonal dune.

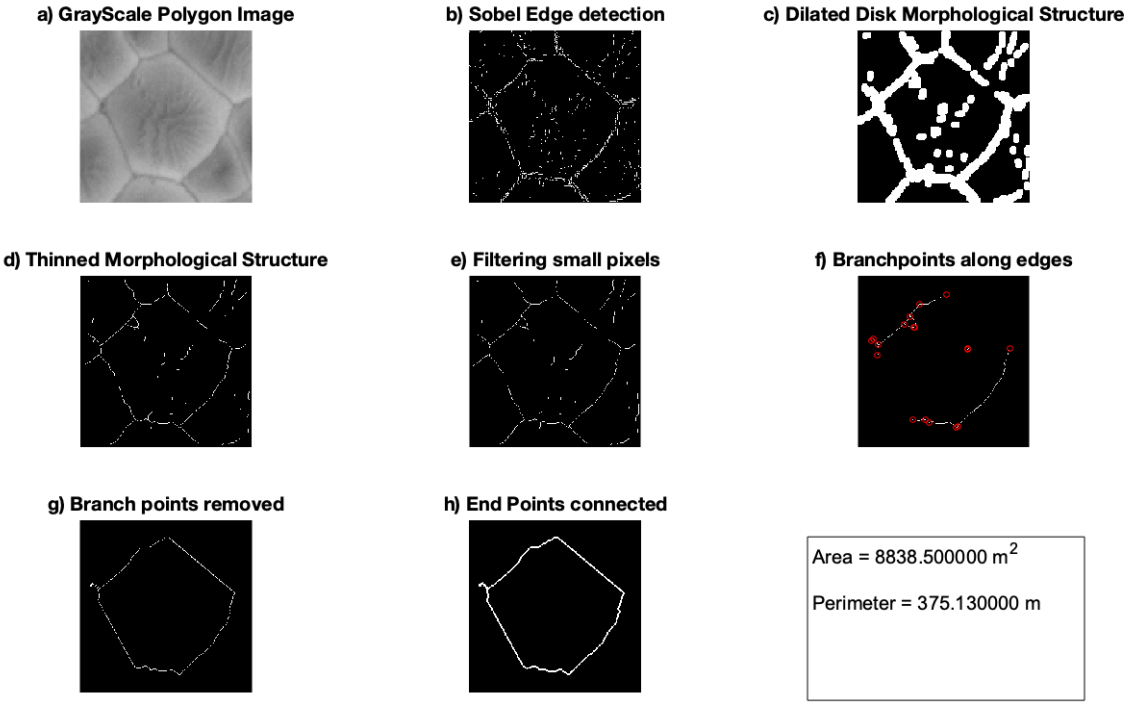

414

415 **Fig. 9.** a) Scale factor 10 zoomed-in HiRISE image of a Martian polygonal dune; b) Sobel edge
416 detection algorithm applied to binary image to determine edges; c) Dilated disk along the edge
417 morphological structure; d)Thinning the morphological structure; e) Filtering disconnected
418 isolated pixels (heuristics); f) Branch points determined; g) Branch points removed; and h) End
419 points connected to trace polygon. Perimeter and area of polygon measured are shown in the
420 bottom-right box.

421

422 The image processing framework developed to characterize the branch points in the polygons
423 of Mars, can equivalently be applied to the analysis of polygons on the Boulby mine walls.
424 Repeated observations over a wider temporal resolution of these polygons would provide us an
425 insight to the evolution of these features. Figure 10 shows the sequence of operations performed
426 by the image processing framework on a point cloud of the polygon.

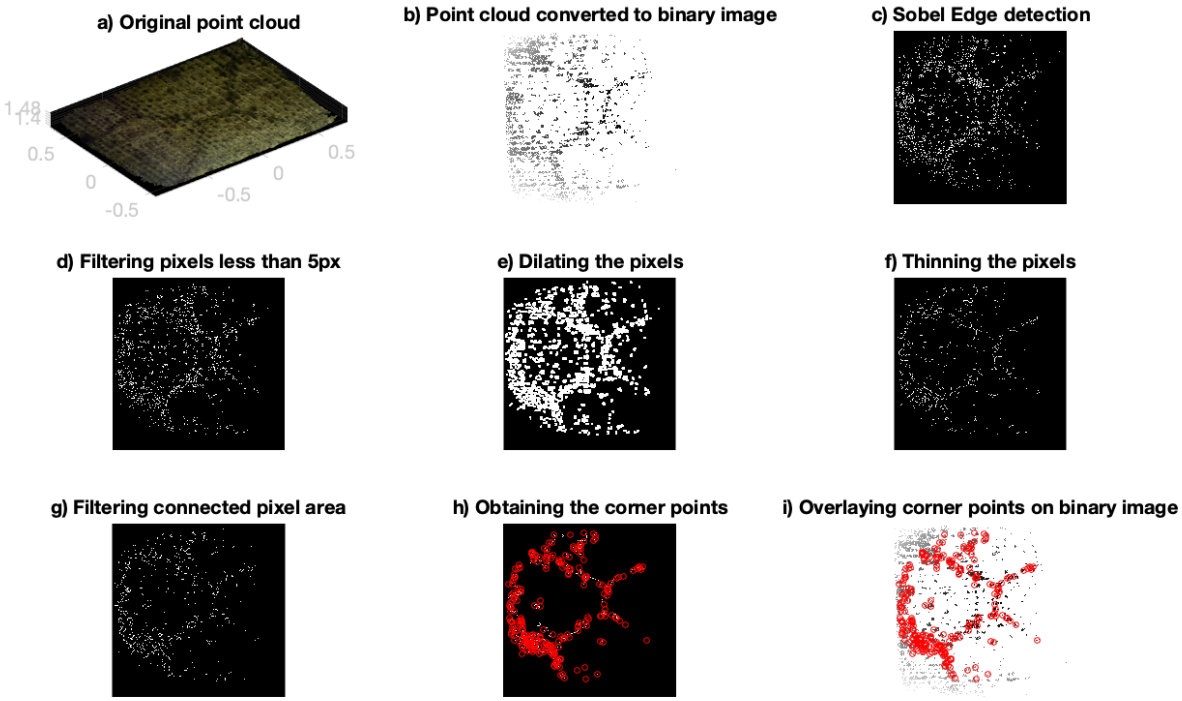

Fig. 10. Image processing framework to obtain the corner points in the polygon point cloud. a) the original point cloud image in RGB; b) filtered point cloud converted to binary image with only RGB pixels greater than the mean of entire point cloud RGB; c) Sobel edge detection algorithm used to capture edges; d) filtering isolated pixels (heuristics); e) dilating the filtered pixels; f) thinning the dilated pixels; g) filtering the connected pixels in binary image; h) obtaining the corner points in the polygon indicated in red; and i) Overlaying the corner points over the binary image of the polygons.

The current framework utilises heuristics to determine the disconnected pixels which limits the framework to polygons with well-defined sharp boundaries. This limitation can be overcome by utilizing Convolutional Neural Network (CNN). CNN's high dimensionality offers the prospect for merging the CNN algorithm with 3D mapping algorithm such as Kintinuous to permit the inclusion and extraction of spectral data from the depth point cloud. Deep learning techniques and CNN can be exploited to obtain a detailed topographical study of such features over a wider spatial and temporal resolution. A CNN based approach using HiRISE images to study geological landforms of Mars, primarily volcanic rootless cones and transverse aeolian ridges has been discussed by (Palafox et al., 2017). Similarly, a rapid machine learning based approach to extract and measure ice wedge polygons from high resolution DTM generated by

446 airborne lidar survey using CNN has been put forth by (Abolt et al., 2019). The application of
447 deep learning CNN for edge detection can provide a powerful tool for surface and subsurface
448 geomorphological exploration of planetary bodies with stereoscopic depth cameras. Polygonal
449 features found on Mars underlain by ice heightens interest in life-detection as their close
450 looking terrestrial ice wedge polygons found in the arctic have been found to contain a higher
451 amount of culturable respiring microorganisms compared to other ice-bearing habitats
452 (Wilhelm et al., 2012). The is of great interest from an astrobiology perspective as these water-
453 bearing habitats could have harboured extant life on Mars.
454
455 ***Long Range Mapping and Localization with InXSpace 3D***
456
457 A long range 3D mapping of the mine shaft was also performed to test the consistency of the
458 InXSpace 3D system over longer distances. The RTAB-Map algorithm was used in this test
459 rather than the Kintinuous algorithm owing to the poor volumetric estimation as the camera is
460 subjected to rotational estimation error and tangential drifting of camera pose. This limitation
461 of Kintinuous algorithm restricts its application to mapping along a single plane. However, a
462 novel algorithm based on Iterative Closest Point (ICP) scheme has been proposed by (Ren et
463 al., 2019) which can account for the tangential drifting and erroneous rotational estimations due
464 to input device errors and these can be incorporated into the existing Kintinuous algorithm.
465 Figure 11 shows the 3D point cloud image of the mine shaft made by KORE as it traversed a
466 length of 10m with the path marked with tapes and the end point marked with a stone. While
467 the striped tape line would obviously not exist on a planetary context, other naturally formed
468 features (like ground cracks or limiting regions with contrasting albedo) may be followed
469 similarly and autonomously.
470

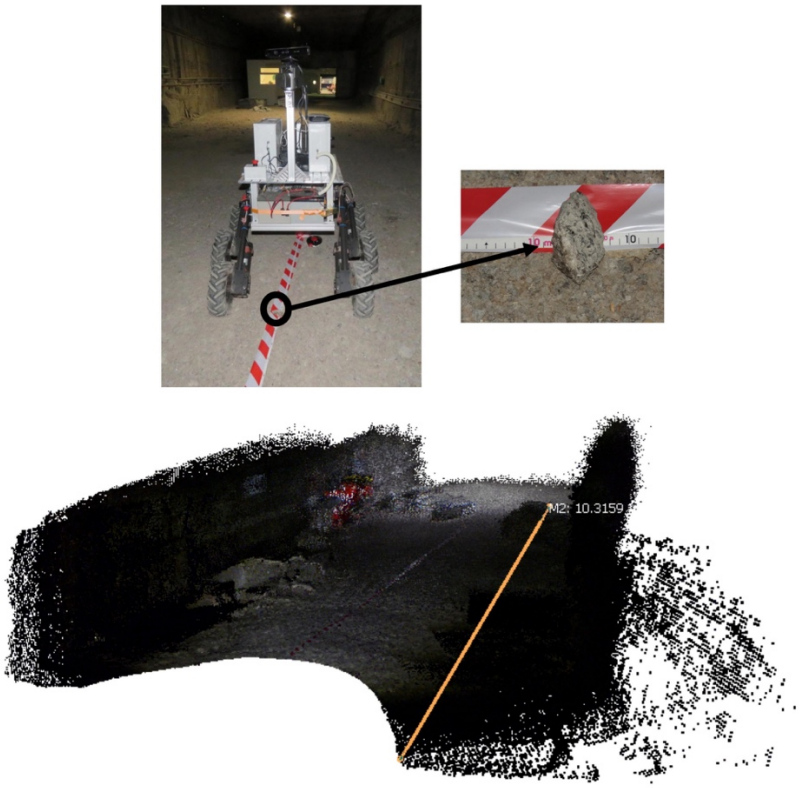

Fig. 11. The image on the top shows KORE following a marked traversal path of 10 m. The image below shows the long-range mapping point cloud of the mine shaft generated by using the RTAB-Map algorithm. The absence of points in a semi-circle pattern in the lower part of the point cloud indicate the shadow zone of KORE.

From the first point on the point cloud to the point representing the stone, the distance could be observed to be approximately 10 m. This test shows that the InXSpace 3D can be used as a viable system to generate local maps of subsurface environments which is a pre-requisite for autonomous navigation in remote environments. The 6 Degree of Freedom (DOF) camera odometry estimation along with the novel GPU-based implementation of an existing dense RGB-D visual odometry algorithm and an advanced fused real-time surface coloring of the Kintinuous algorithm for spatially extended KinectFusion enables a robust tracking along with RGB-D mapping (Whelan et al., 2012). Localization is beneficial for Rover navigation especially in places like subsurface environments where there is an absence of Global Positioning System (GPS) signal reception. The use of depth camera for localization have been elucidated by (Li and Li, 2014 and Biswas and Veloso, 2012). The localization data from the

pose graph estimates of the InXSpace 3D system can be exploited to create autonomous navigation paths for future exploration rovers after a primary rover such as KORE has scanned the subsurface environment and created a 3D point cloud map. Figure 12 shows the traversal path of KORE from the localization data obtained from the pose graph of the Kinect camera.

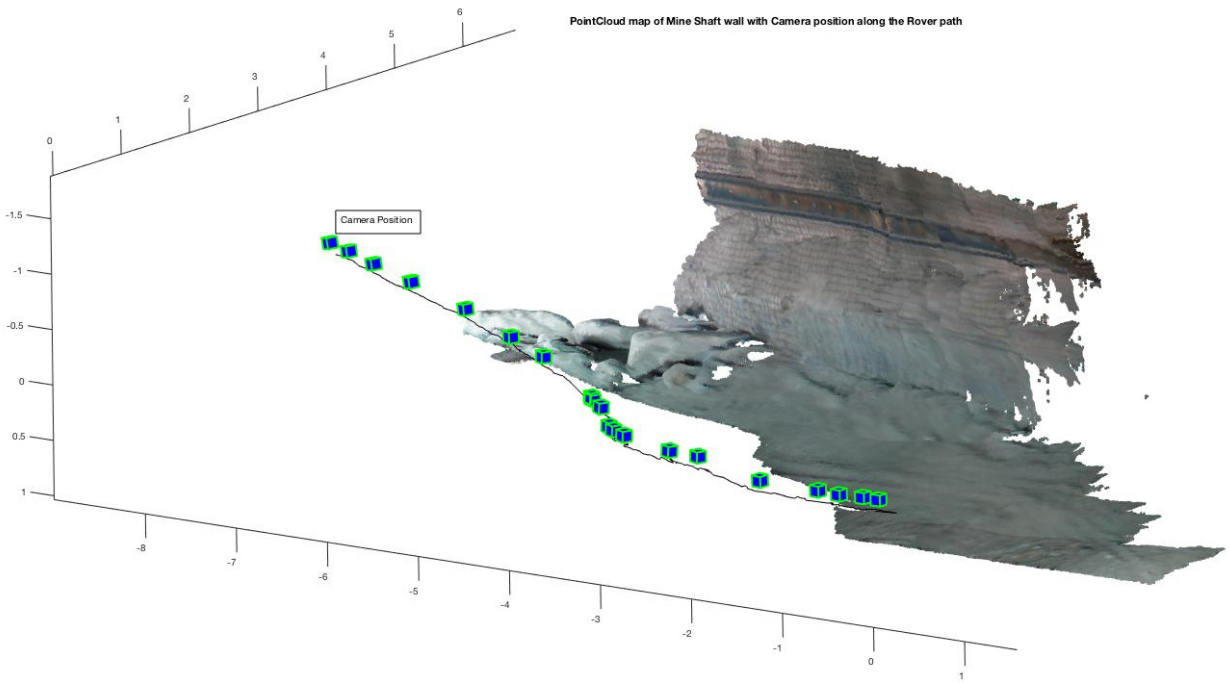

Fig. 12. Rover path with the camera position obtained from the pose graph data obtained through the Kintinuous algorithm during mapping of the mine shaft walls.

Mine Safety with InXSpace 3D

Along with the mapping capability of the InXSpace 3D system for geomorphological studies, the system was tested for its applicability to mine safety. The synergy between mining and analogue studies for planetary exploration is one of the fundamental drivers for the MINAR campaigns (Payler et al., 2016) which emphasizes technology transfer between both fields. The InXSpace 3D on KORE was utilized in demonstrating mine safety by mapping a miner in complete pitch-black darkness. This test showed that InXSpace 3D could be a viable tool for

identifying miners who are trapped in the mine due to mine shaft wall collapse or other hazardous scenarios. By close range mapping, the facial features from the 3D point cloud could be obtained to account for the trapped person. Figure 13 shows the 3D point cloud image of a miner sitting on a rock down in the mine shaft.

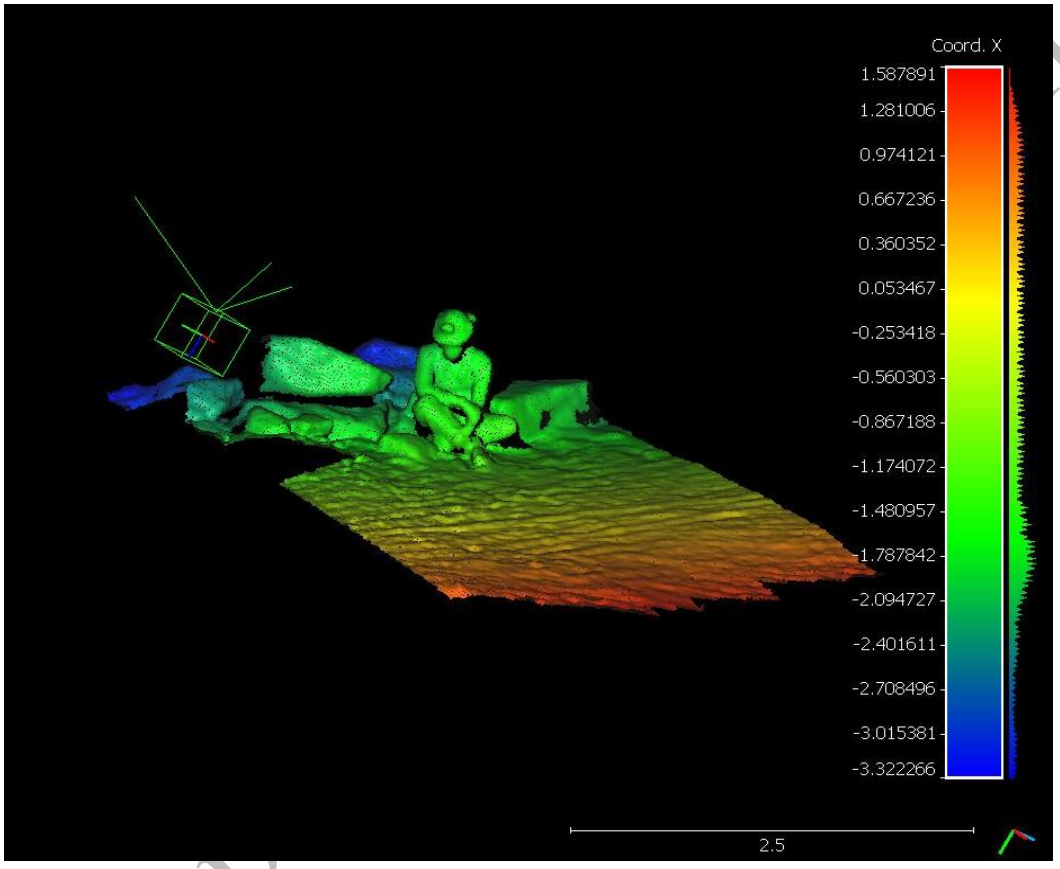

Fig. 13. 3D reconstruction of a miner sitting on a rock in the Boulby mine with the green box indicating the position of the camera as the KORE rover approached him. The scale bar is in m.

Moreover, the InXSpace 3D system can be used as an inspection tool to analyse safety features in the mine shaft. Figure 14 indicates a snap in the metal frame against the mine wall that occurred due to compressive forces acting along the mine shaft walls. The advantage of having a 3D point cloud of the failure part in close range mapping rather than a 2D image is that the point cloud analysis allows a precise monitoring of the dimensions of failures in such hazardous regions to ensure that these regions do not grow over a period of time. Also, from the point

cloud image, we can observe that the bolts that hold the metal frames to the mine shaft walls are clearly visible, which can allow a remote monitoring of these critical components. Manual inspection of these critical elements using traditional visual methods is time-consuming, laborious and prone to human factor errors. Robotic exploration is a viable option that reduces inspection time and can account for reduced errors. Image processing with RGB image data sets using deep learning have been discussed by Huang, Li and Zhang (2018). However, utilizing 3D point cloud data for such inspection supersedes the use of 2D images (Koch and Brilakis, 2011a). The 3D point cloud data generated from the RGB-D camera using the SLAM algorithms can also be exploited for such automatic detection of missing bolts or anomalies by incorporating neural networks as proposed in detecting the polygonal geomorphological features. The synergistic application is not only limited to terrestrial mining but could also be used a crucial safety assessment tool to analyse unknown subsurface extra-terrestrial environments especially during human space exploration.

Fig. 14. (left) RGB image of the metal frame failure detected and (right) shows the 3D point cloud of the failure. Also, the bolts along the metal frame are visible in the point cloud data.

Astrobiology experiments

Subsurface environments span the entire solar system with every planetary body being unique. Subsurface oceans have been found to exist on the moons of Jupiter such as Ganymede, Callisto, Europa and Saturnian moons such as Enceladus and Titan, and there are other bodies in the solar system where possible subsurface ocean could exist. The presence of these subsurface oceans further raises the question of life in them. Apart from the presence of subsurface oceans on the icy moons, subsurface environments of rocky planet such as Mars are proposed to have had the right conditions to host life (Tarnas et al., 2018). The intense UV radiation bombarding the planet, low pressures close to the triple point of water, oxidizing perchlorate rich soil and cold freezing temperatures provide an inhospitable scenario for life to exist on the surface of Mars. Unlike the surface of Mars, the subsurface of Mars is expected to have a higher pressure (Schuerger et al., 2013), shielding from intense UV irradiation and galactic cosmic rays, a stable temperature (Fisk and Giovannoni, 1999), and potentially the presence of subglacial liquid water (Orosei et al., 2018) which provides an ideal scenario to host life. A study made by Michalski et al. (2017), suggested that life could exist in the subsurface of Mars up to 8 km. A detailed study on the subsurface habitability of Mars was done by Cockell (2014). Methane detected on Mars, raises question of whether it could be from biotic or abiotic sources. One of the hypotheses is that methane could be produced by the methanogens in the subsurface of Mars. During the MINAR 5 campaign, methane analysis was performed at 13 locations in the mine tunnel shafts and it was found that the methane concentrations at few places reached above 100 ppm (Cockell et al., 2018). The presence of these methane concentrations may represent the partial trapping of upwelling thermogenic methane found concentrated within certain mineral layers like potash. However, in a study by Fernández-Remolar et al. (2008) of underground habitats in the Rio Tinto Basin, Spain, methane could be detected between 13 to 34 ppm in one of the boreholes dug, with an inverse correlation with hydrogen signifying the presence of methanogenesis. During the MINAR6

campaign, KORE was fitted with a laser absorption spectroscopy-based methane detector on a linear actuator which could detect methane plumes from about a distance of up-to 50 m. The setup could be controlled remotely to scan an area of interest using the rover locomotion and linear actuator-based platform. A technological demonstration of the setup was performed by simulating a methane plume from under a rock rubble as shown in the Figure 15 by releasing methane from an aluminium coated Tedlar bag. Issues with logistics prevented rover access to the sites explored in MINAR5 campaign with methane produced by thermogenic activity.

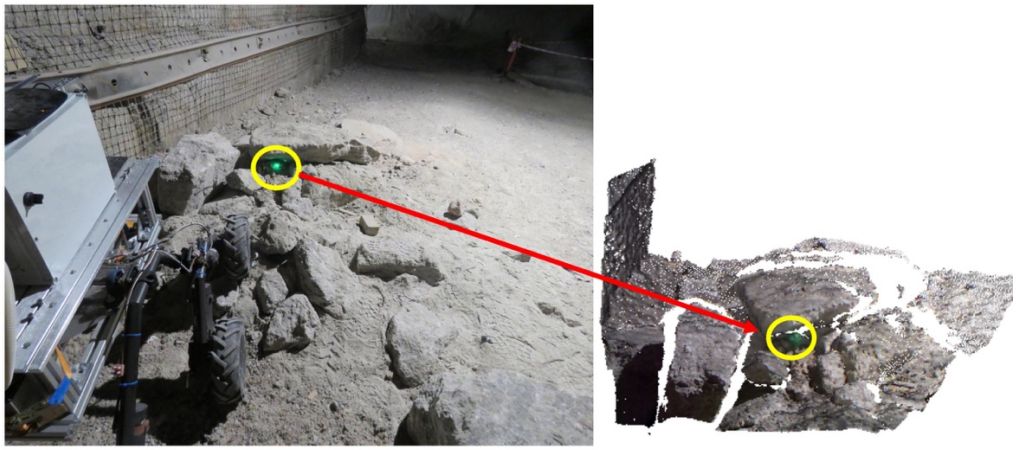

Fig. 15. (left) KORE pointing the laser methane detector at a simulated methane plume created with a methane packet placed under the rock rubble; (right) 3D point cloud of the rock rubble with the green point indicating the laser impingement point.

The use of such remote methane monitoring instrument with a long detection range of 50m to detect methane satisfies the application to preliminary astrobiology studies and mine safety. The laser-based methane detector is limited in sensitivity to 5ppm and cannot determine the C and H stable isotopes which are of interest to study the source of the methane. The laser-based methane detector can be substituted with a more sophisticated hyperspectral imager. Hyperspectral imagers are a great tool to remotely monitor the hydrocarbon emissions along with gases such as carbon monoxide, carbon dioxide, nitrogen dioxide and hydrogen sulphide. These gases are of biological significance and scanning potential habitats such as polygonal

structures can provide an insight to the biosignature detection in such closed environments. The use of such remote monitoring instruments provide a very flexible platform to study locations which are quite inaccessible. The remote gas detection techniques on rovers enhances mine safety operations, as these detectors can be used to scan a potential hazardous location from a safe distance rather than a close encounter.

Environmental sensors

KORE is fitted with an environmental station that measures atmospheric parameters such as temperature, humidity, pressure along with various gases such NO_2, SO_2, H_2S, CO, CO_2, O_3, O_2, formaldehyde, volatile organic compounds and particulates. The environmental station was operated for a quite a short period of time (22 hrs) due to operational limitations, especially with the limited battery capacity and hence some of the electrochemical sensors such as the ones measuring CO, O_3, SO_2, NO_2, H_2S and volatile organic compounds failed to stabilize within this interval of time. The data obtained from the temperature, humidity, pressure, CO_2, O_2 and formaldehyde sensors are shown in the following plot, Figure 16. The first two hours of data can be neglected to account for the time required for the sensors to stabilize.

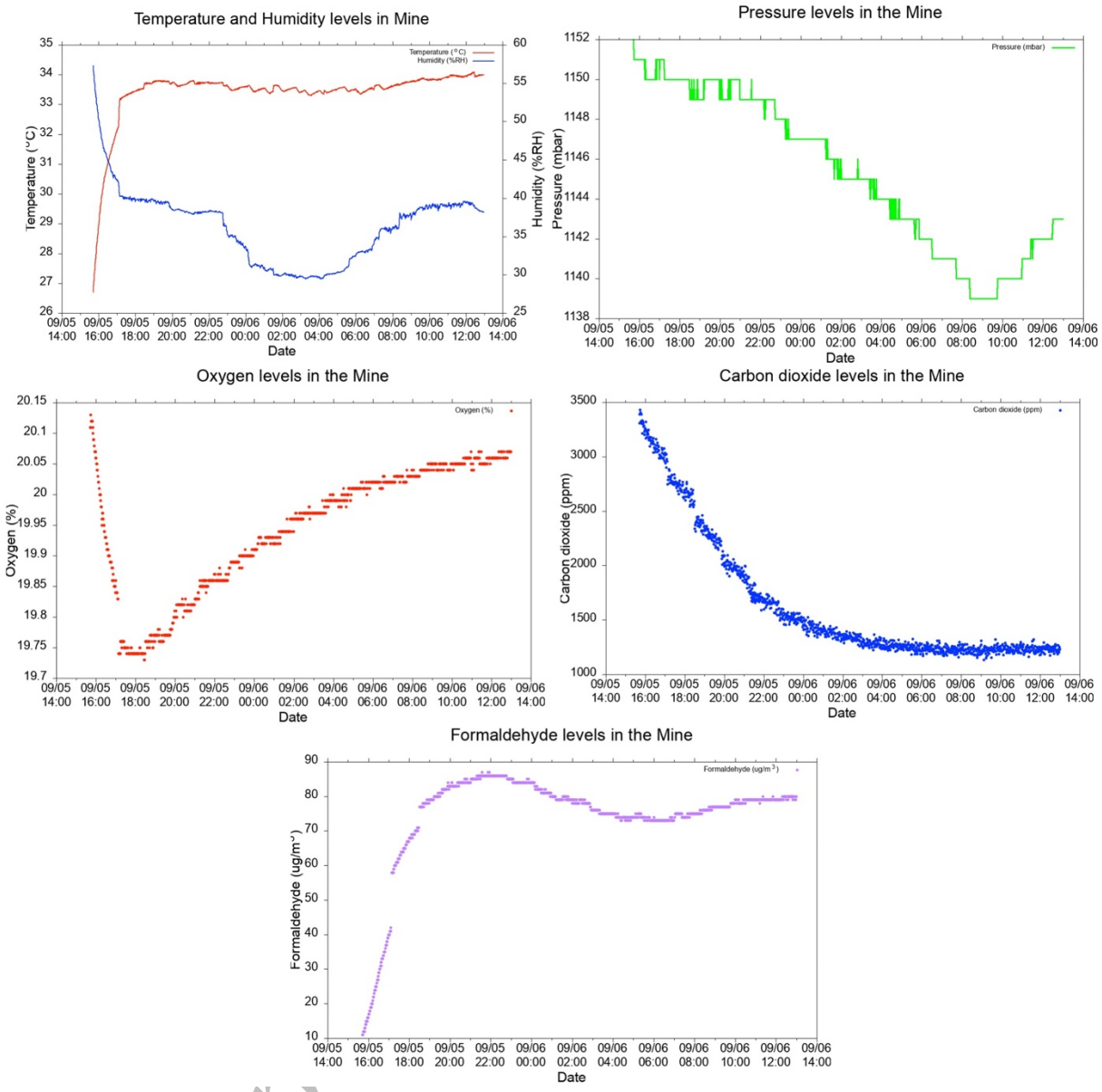

603

604 **Fig. 16.** Plots obtained from the data of the Environmental sensors aboard KORE rover
605 operating over a span of 22 hours. The initial 2 hours are neglected to account for the sensor
606 warm up time.

607

608 The mean carbon dioxide levels in the mine are above 1000ppm which is expected owing to
609 the presence of an indoor environment down in the mine shafts. The most interesting
610 observation from the gas measurements was the levels of formaldehyde present in the mine.
611 During the 22 hrs of operation of the environmental station, we could observe an average
612 formaldehyde concentration of 78.5 $\mu g/m^3$ which is well within the safe exposure levels as with
613 concentration of above 100 $\mu g/m^3$, formaldehyde has been associated with irritation to the eyes,

skin, nose, and throat, however there is a substantial variation in individual responses (WHO, 2000). Hence monitoring the formaldehyde levels is very important in enclosed environments such as mines where the dilution of these gases with the ambient air is restricted and is very crucial for the occupational health of the miners. Formaldehyde has also a strong implication in extra-terrestrial environments as a prebiotic chemical (Cleaves II, 2008, Kitadai and Maruyama, 2018) and hence monitoring this or other potentially relevant prebiotic or life-related volatiles is very useful for astrobiology (Blair, Magnani, Brand and Wouterloot, 2008).

Conclusion

The KORE rover has been built as a technological demonstration for analogue exploration of subsurface environments. For this purpose, it has been completely designed using Commercial Off the Shelf (COTS) components and thus none of the components used in the rover are still flight qualified. Technical demonstrators allow to test and show the scientific application of a payload while estimating the power consumption, volume, weight etc. needs and finding the most important functional requirements that limit or allow operability. These low Technological Readiness Level (TRL) prototypes are the first step required to build space exploration spacecrafts and/or payloads. During the MINAR6 campaign, a number of observations were implemented using KORE as an autonomous laboratory rover with instrumentation that is used to validate certain hypothesis. The rover campaign lasted 6 days with a total experimentation time of ~22 hours. As a hypothesis driven campaign, the MINAR 6 served as an ideal scenario to validate the hypothesis of using a low-cost subsurface rover platform with low-cost mapping technologies to capture point clouds of both man-made artificial features and naturally occurring polygons on the polyhalite roofs of the mine. The methodology incorporated in the mapping with InXSpace 3D system coupled with machine

learning and CNN can be exploited for future surface and subsurface robotic explorations to obtain a more vivid study of the geomorphological features.

The 3D point cloud data generated using the Kintinuous algorithm can also be utilized to perform inspection of critical elements such as bolts in the mine shafts and with deep learning incorporated, their inspection capability can be further enhanced. The localization information obtained from the mapping algorithms can be used to create a local map of the environment, which would provide an automated navigation capability to the rover. This would help the rover traverse a relatively plain terrain without encountering large boulders and debris. The study of the volatile accumulation in the mine has also been validated from an astrobiological point of view, using a methane detection payload and environmental station to measure formaldehyde concentrations, which is crucial to the occupational health of the miners. This study demonstrates that a low-cost, robust remotely operable subsurface platform can be used for geomorphology, astrobiology and mining study and it has been successfully validated by utilizing KORE.

Acknowledgment

The authors of this paper would like to thank Kempe Foundation for its generous funding support to develop KORE, the workshop at the Teknikens Hus, Luleå, for their invaluable and unconditional support in helping with the fabrication of the KORE components and the organizers of the MINAR campaign comprising the UK Centre of Astrobiology, ICL Boulby Mine and STFC Boulby Underground Laboratory, UK. MPZ has been partially funded by the Spanish State Research Agency (AEI) Project No. MDM-2017-0737 Unidad de Excelencia "María de Maeztu"- Centro de Astrobiología (INTA-CSIC).

References

Abbott, S. (2016) *Depositional architecture and facies variability in anhydrite and polyhalite sequences: a multi-scale study of the Jurassic (Weald Basin, Brightling Mine) and Permian (Zechstein Basin, Boulby Mine) of the UK.* Ph.D Thesis. Imperial College London. Available at: https://spiral.imperial.ac.uk/bitstream/10044/1/45720/1/Abbott-S-2016-PhD-Thesis.pdf (Accessed: 01 January 2020).

Abolt, C., Young, M., Atchley, A. and Wilson, C. (2019). Brief communication: Rapid machine-learning-based extraction and measurement of ice wedge polygons in high-resolution digital elevation models. The Cryosphere, 13(1), pp.237-245.

Altuntas, N., Uslu, E., Cakmak, F., Amasyali, M. and Yavuz, S. (2017). Comparison of 3-dimensional SLAM systems: RTAB-Map vs. Kintinuous. 2017 International Conference on Computer Science and Engineering (UBMK).

Bethke, C. (1990). Brine Migrations Across North America: The Plate Tectonics of Groundwater. Annual Review of Earth and Planetary Sciences, 18(1), pp.287-315.

Blair, S., Magnani, L., Brand, J. and Wouterloot, J., 2008. Formaldehyde in the Far Outer Galaxy: Constraining the Outer Boundary of the Galactic Habitable Zone. Astrobiology, 8(1), pp.59-73.

Biswas, J. and Veloso, M. (2012). Depth camera based indoor mobile robot localization and navigation. 2012 IEEE International Conference on Robotics and Automation.

689

690 Bowler, S (2013) From outer space to mining. Astronomy and Geophysics 54, 3.1.–33.3.

691

692 Butler D.A. (1995) Zoogeomorphology: Animals as Geomorphic Agents, Cambridge
693 University Press, Cambridge, UK.

694

695 Cady S.L. and Noffke N. (2009) Geobiology: evidence for early life on Earth and the search
696 for life on other planets. GSA Today 19:4–10.

697

698 Christiansen, E. H., J. A. Hopler, Geomorphic evidence for subsurface volatile reservoirs in the
699 Elysium region of Mars (abstract), Lunar and Planetary Science, , XVII, 125–126, Lunar
700 and Planetary Institute, Houston, 1986.

701

702 Cleaves II, H., 2008. The prebiotic geochemistry of formaldehyde. Precambrian Research,
703 164(3-4), pp.111-118.

704

705 Cockell, Charles. (2014). The subsurface habitability of terrestrial rocky planets: Mars.

706

707 Cockell, C, Holt, J, Campbell, J, Groseman, H, Josset, J, Bontognali, T, Phelps, A, Hakobyan,
708 L, Kuretn, L, Beattie, A, Blank, J, Bonaccorsi, R, McKay, C, Shirvastava, A, Stoker, C,
709 Willson, D, McLaughlin, S, Payler, S, Stevens, A, Wadsworth, J, Bessone, L, Maurer, M,
710 Sauro, F, Martin-Torres, J, Zorzano, M, Bhardwaj, A, Soria-Salinas, A, Mathanlal, T,
711 Nazarious, M, Ramachandran, A, Vaishampayan, P, Guan, L, Perl, S, Telling, J,
712 Boothroyd, I, Tyson, O, Realff, J, Rowbottom, J, Lauernt, B, Gunn, M, Shah, S, Singh,
713 S, Paling, S, Edwards, T, Yeoman, L, Meehan, E, Toth, C, Scovell, P and Suckling, B

(2018) Subsurface scientific exploration of extraterrestrial environments (MINAR 5): analogue science, technology and education in the Boulby Mine, UK. International Journal of Astrobiology 18(2), 157–182. https://doi.org/10.1017/S1473550418000186

Corenblit, D., Darrozes, J., Julien, F., Otto, T., Roussel, E., Steiger, J. and Viles, H. (2019). The Search for a Signature of Life on Mars: A Biogeomorphological Approach. Astrobiology, 19(10), pp.1279-1291.

De Sanctis, M., Altieri, F., Ammannito, E., Biondi, D., De Angelis, S., Meini, M., Mondello, G., Novi, S., Paolinetti, R., Soldani, M., Mugnuolo, R., Pirrotta, S., Vago, J. and the Ma_MISS team (2017). Ma_MISS on ExoMars: Mineralogical Characterization of the Martian Subsurface. Astrobiology, 17(6-7), pp.612-620.

Dromart G., Quantin C., and Broucke O. (2007) Stratigraphic architectures spotted in southern Melas Chasma, Valles Marineris, Mars. Geology 35:363–366.

Dundas, C.M., Bramson, A.M., Ojha, L., Wray, J.J., Mellon, M.T., Byrne, S., McEwen, A.S., Putzig, N.E., Viola, D., Sutton, S., Clark, E., and Holt, J.W. (2018) Exposed subsurface ice sheets in the Martian mid-latitudes. Science 359:199–201.

Fernández-Remolar, D., Prieto-Ballesteros, O., Rodríguez, N., Gómez, F., Amils, R., Gómez-Elvira, J. and Stoker, C. (2008). Underground Habitats in the Río Tinto Basin: A Model for Subsurface Life Habitats on Mars. Astrobiology, 8(5), pp.1023-1047.

738 Fisk, M. and Giovannoni, S. (1999). Sources of nutrients and energy for a deep biosphere on
739 Mars. Journal of Geophysical Research: Planets, 104(E5), pp.11805-11815.
740
741 Gorbushina A.A., Krumbein W.E., and Volkmann M. (2004) Rock surfaces as life indicators:
742 new ways to demonstrate life and traces of former life. Astrobiology 2:203–213.
743
744 Grant, J., Irwin, R., Grotzinger, J., Milliken, R., Tornabene, L., McEwen, A., Weitz, C.,
745 Squyres, S., Glotch, T. and Thomson, B. (2008). HiRISE imaging of impact megabreccia
746 and sub-meter aqueous strata in Holden Crater, Mars. Geology, 36(3), p.195.
747
748 Grotzinger J., Bell J.III, Herkenhoff K., Johnson J., Knoll A., McCartney E., McLennan S.,
749 Metz J., Moore J., Squyres S., Sullivan R., Aharonson O., Arvidson R., Joliff B.,
750 Golombek M., Lewis K., Parker T., and Soderblom J. (2006) Sedimentary textures
751 formed by aqueous processes, Erebus crater, Meridiani Planum, Mars. Geology 34:1085–
752 1088.
753
754 Huang, H., Li, Q. and Zhang, D. (2018). Deep learning based image recognition for crack and
755 leakage defects of metro shield tunnel. Tunnelling and Underground Space Technology,
756 77, pp.166-176.
757
758 Jacob C. Yde, Teresa G. Bárcena and Kai W. Finster (September 12th, 2011). Subglacial and
759 Proglacial Ecosystem Responses to Climate Change, Climate Change Juan Blanco and
760 Houshang Kheradmand, IntechOpen, DOI: 10.5772/24236.
761

J. J. Plaut, A. Safaeinili, J. W. Holt, R. J. Phillips, J. W. Head III, R. Seu, N. E. Putzig, A. Frigeri, Radar evidence for ice in lobate debris aprons in the mid-northern latitudes of Mars. Geophys. Res. Lett. 36, L02203 (2009). doi:10.1029/2008GL036379.

Kitadai, N. and Maruyama, S., 2018. Origins of building blocks of life: A review. Geoscience Frontiers, 9(4), pp.1117-1153.

Koch, C., Brilakis, I. (2011a). "Pothole Detection in Asphalt Pavement Images." J. of Advanced Engineering Eng. Informatics, 25(3), 507–515.

Labbé, M. and Michaud, F. (2018). RTAB-Map as an open-source lidar and visual simultaneous localization and mapping library for large-scale and long-term online operation. Journal of Field Robotics, 36(2), pp.416-446.

Lewis K., Aharonson O., Grotzinger J., Kirk R., McEwen A., and Suer T. (2008) Quasi-periodic bedding in the sedimentary rock record of Mars. Science 322:1532–1535.

L. R. Dartnell, L. Desorgher, J. M. Ward, A. J. Coates. Martian sub-surface ionising radiation: biosignatures and geology. Biogeosciences Discussions, European Geosciences Union, 2007, 4 (1), pp.455-492.

Li, R. and Li, Y. (2014). Localization of leader-follower formations using kinect and RTK-GPS. 2014 IEEE International Conference on Robotics and Biomimetics (ROBIO 2014).

Lim, D., Abercromby, A., Kobs Nawotniak, S., Lees, D., Miller, M., Brady, A., Miller, M., Mirmalek, Z., Sehlke, A., Payler, S., Stevens, A., Haberle, C., Beaton, K., Chappell, S., Hughes, S., Cockell, C., Elphic, R., Downs, M. and Heldmann, J., 2019. The BASALT Research Program: Designing and Developing Mission Elements in Support of Human Scientific Exploration of Mars. Astrobiology, 19(3), pp.245-259.

Lucchita, B. K. (1983), Permafrost on Mars: Polygonally fractures ground, in Permafrost: Fourth International Conference Proceedings, Natl. Acad. Press, Washington, D. C.

Malin, M. (2000). Sedimentary Rocks of Early Mars. Science, 290(5498), pp.1927-1937.

Malin, M. and Edgett, K. (2001). Mars Global Surveyor Mars Orbiter Camera: Interplanetary cruise through primary mission. Journal of Geophysical Research: Planets, 106(E10), pp.23429-23570.

Malin M.C. and Edgett K.S. (2003) Evidence for persistent flow and aqueous sedimentation on early Mars. Science 302:1931–1934.

Mangold, N. (2005), High latitude patterned grounds on Mars: Classification, distribution and climatic control, Icarus, 174, 336–359, doi:10.1016/j.icarus.2004.07.030.

Martín-Torres, J, Olsson P, Zorzano, M, Bhardwaj, A, Sam, L, and Singh, S 2020, 'Martian caves as special region candidates', *LPI Third International Planetary Caves Conference*, San Antonio, Texas, USA,18th-21th February, 2020.

Mary Beth Wilhelm, Charles S Cockel, Scott Perl, Jennifer Wadsworth, Sam Payler, Sean Paling, Thomas Edwards, Sean McMahon, (2019) Lipid Biomarker Content in 0.25 Ga Boulby Mine Salt Deposit & Implications for Mars, Astrobiology Science Conference, Bellevue, Washington, 24-28 June 2019.

Mathanlal, T., Bhardwaj, A., Vakkada Ramachandran, A., Zorzano, M., Martín-Torres, J., Cockell, C., Paling, S. and Edwards, T. (2019). Subsurface robotic exploration for geomorphology, astrobiology and mining during MINAR6 campaign, Boulby Mine, UK: part I (Rover development). International Journal of Astrobiology, pp.1-16.

Michalski, J.R.; Onstott, T.C.; Mojzsis, S.J.; Mustard, J.; Chan, Q.H.S.; Niles, P.B.; Johnson, S.S. The Martian subsurface as a potential window into the origin of life. Nat. Geosci. 2018, 11, 21–26.

Milliken R.E., Grotzinger J.P., and Thomson B.J. (2010) Paleoclimate of Mars as captured by the stratigraphic record in Gale Crater. Geophys Res Lett 37:4.

Mutch, T. A., R. E. Arvidson, J. W. Head, K. L. Jones, and R. S. Sainders (1976), The Geology of Mars, Princeton Univ. Press, Princeton, NJ.

Mutch, T. A., R. E. Arvidson, A. B. Binder, E. A. Guinness, and E. C. Morris (1977), The geology of the Viking Lander 2 site, J. Geophys. Res., 82(28), 4452–4467, doi:10.1029/JS082i028p04452.

835 Naylor L.A. (2005) The contributions of biogeomorphology to the emerging field of
836 geobiology. Palaeogeogr Palaeoclimatol Palaeoecol 219:35–51.
837
838 Noffke N., Christian D., Wacey D., and Hazen R.M. (2013) Microbially induced sedimentary
839 structures recording an ancient ecosystem in the ca. 3.48 billion-year-old Dresser
840 Formation, Pilbara, Western Australia. Astrobiology 13:1103–1124.
841
842 Noffke N. (2014) Ancient sedimentary structures in the <3.7 Ga Gillespie Lake Member, Mars,
843 that resemble macroscopic morphology, spatial associations, and temporal succession in
844 terrestrial microbialites. Astrobiology 15:169–192. Medline.
845
846 Oliver, J. (1986). Fluids expelled tectonically from orogenic belts: Their role in hydrocarbon
847 migration and other geologic phenomena. Geology, 14(2), p.99.
848
849 Orosei, R., Lauro, S., Pettinelli, E., Cicchetti, A., Coradini, M., Cosciotti, B., Di Paolo, F.,
850 Flamini, E., Mattei, E., Pajola, M., Soldovieri, F., Cartacci, M., Cassenti, F., Frigeri, A.,
851 Giuppi, S., Martufi, R., Masdea, A., Mitri, G., Nenna, C., Noschese, R., Restano, M. and
852 Seu, R. (2018). Radar evidence of subglacial liquid water on Mars. Science, p.eaar7268.
853
854 Palafox, L., Hamilton, C., Scheidt, S. and Alvarez, A. (2017). Automated detection of
855 geological landforms on Mars using Convolutional Neural Networks. Computers &
856 Geosciences, 101, pp.48-56.
857
858 Payler, S., Biddle, J., Coates, A., Cousins, C., Cross, R., Cullen, D., Downs, M., Direito, S.,
859 Edwards, T., Gray, A., Genis, J., Gunn, M., Hansford, G., Harkness, P., Holt, J., Josset,

J., Li, X., Lees, D., Lim, D., Mchugh, M., Mcluckie, D., Meehan, E., Paling, S., Souchon, A., Yeoman, L. and Cockell, C. (2016). Planetary science and exploration in the deep subsurface: results from the MINAR Program, Boulby Mine, UK. International Journal of Astrobiology, 16(2), pp.114-129.

Pechmann, J. C. (1980), The origin of polygonal troughs on the northern plains of Mars, Icarus, 42, 185–210.

Picardi, Giovanni & Plaut, Jeffrey & Biccari, Daniela & Bombaci, Ornella & Calabrese, Diego & Cartacci, Marco & Cicchetti, A. & Clifford, Stephen & Edenhofer, Peter & Farrell, William & Federico, Costanzo & Frigeri, Alessandro & Gurnett, Donald & Hagfors, Tor & Heggy, Essam & Herique, A. & Huff, Richard & Ivanov, Anton & Johnson, William & Zampolini, Enrico. (2006). Radar Soundings of the Subsurface of Mars. Science (New York, N.Y.). 310. 1925-8. 10.1126/science.1122165.

Ren, B., Wu, J., Lv, Y., Cheng, M. and Lu, S. (2019). Geometry-Aware ICP for Scene Reconstruction from RGB-D Camera. Journal of Computer Science and Technology, 34(3), pp.581-593.

Rummel, J., Beaty, D., Jones, M., Bakermans, C., Barlow, N., Boston, P., Chevrier, V., Clark, B., de Vera, J., Gough, R., Hallsworth, J., Head, J., Hipkin, V., Kieft, T., McEwen, A., Mellon, M., Mikucki, J., Nicholson, W., Omelon, C., Peterson, R., Roden, E., Sherwood Lollar, B., Tanaka, K., Viola, D. and Wray, J. (2014). A New Analysis of Mars "Special Regions": Findings of the Second MEPAG Special Regions Science Analysis Group (SR-SAG2). Astrobiology, 14(11), pp.887-968.

Schuerger, A.C.; Ulrich, R.; Berry, B.J.; Nicholson, W.L. Growth of Serratia liquefaciens under 7 mbar, 0 ◦C, and CO2 -enriched anoxic atmospheres. Astrobiology 2013, 13, 115–131.

Seibert, N. M., and J. S. Kargel (2001), Small-scale martian polygonal terrain: Implications for liquid surface water, Geophys. Res. Lett., 28(5), 899–902, doi:10.1029/2000GL012093.

Tarnas, J., Mustard, J., Sherwood Lollar, B., Bramble, M., Cannon, K., Palumbo, A. and Plesa, A. (2018). Radiolytic H2 production on Noachian Mars: Implications for habitability and atmospheric warming. Earth and Planetary Science Letters, 502, pp.133-145.

Trainer, M., Wong, M., McConnochie, T., Franz, H., Atreya, S., Conrad, P., Lefèvre, F., Mahaffy, P., Malespin, C., Manning, H., Martín-Torres, J., Martínez, G., McKay, C., Navarro-González, R., Vicente-Retortillo, Á., Webster, C. and Zorzano, M. (2019). Seasonal variations in atmospheric composition as measured in Gale Crater, Mars. Journal of Geophysical Research: Planets.

Viles H.A., editor. (1988) Biogeomorphology, Blackwell, Oxford, UK.

Wang, X., Xue, Y. and Ma, Y. (2010). Streptohalobacillus salinus gen. nov., sp. nov., a moderately halophilic, Gram-positive, facultative anaerobe isolated from subsurface saline soil. International Journal of Systematic and Evolutionary Microbiology, 61(5), pp.1127-1132.

Wang, X., Xue, Y. and Ma, Y. (2010). Virgibacillus subterraneus sp. nov., a moderately halophilic Gram-positive bacterium isolated from subsurface saline soil. International Journal of Systematic and Evolutionary Microbiology, 60(12), pp.2763-2767.

Warren, J., 1999, Evaporites: Their Evolution and Economics. Blackwell, p. 438.

Webster, C., Mahaffy, P., Atreya, S., Flesch, G., Mischna, M., Meslin, P., Farley, K., Conrad, P., Christensen, L., Pavlov, A., Martin-Torres, J., Zorzano, M., McConnochie, T., Owen, T., Eigenbrode, J., Glavin, D., Steele, A., Malespin, C., Archer, P., Sutter, B., Coll, P., Freissinet, C., McKay, C., Moores, J., Schwenzer, S., Bridges, J., Navarro-Gonzalez, R., Gellert, R. and Lemmon, M. (2014). Mars methane detection and variability at Gale crater. Science, 347(6220), pp.415-417.

Webster, C., Mahaffy, P., Atreya, S., Moores, J., Flesch, G., Malespin, C., McKay, C., Martinez, G., Smith, C., Martin-Torres, J., Gomez-Elvira, J., Zorzano, M., Wong, M., Trainer, M., Steele, A., Archer, D., Sutter, B., Coll, P., Freissinet, C., Meslin, P., Gough, R., House, C., Pavlov, A., Eigenbrode, J., Glavin, D., Pearson, J., Keymeulen, D., Christensen, L., Schwenzer, S., Navarro-Gonzalez, R., Pla-García, J., Rafkin, S., Vicente-Retortillo, Á., Kahanpää, H., Viudez-Moreiras, D., Smith, M., Harri, A., Genzer, M., Hassler, D., Lemmon, M., Crisp, J., Sander, S., Zurek, R. and Vasavada, A., 2018. Background levels of methane in Mars' atmosphere show strong seasonal variations. Science, 360(6393), pp.1093-1096.

Westall F., Foucher F., Bost N., Bertrand M., Loizeau D., Vago J.L., Kminek G., Gaboyer F., Campbell K.A., Bréhéret J.-G., Gautret P., and Cockell C.S. (2015) Biosignatures on

Mars: what, where, and how? Implications for the search for martian life. Astrobiology 15:998–1029.

Whelan, T, McDonald, J, Kaess, M, Fallon, M, Johannsson, H and Leonard, JJ (2012) Kintinuous: Spatially Extended KinectFusion, in RSS Workshop on RGB-D: Advanced Reasoning with Depth Cameras.

Whelan, Thomas; Johannsson, Hordur; Kaess, Michael; Leonard, John J.; McDonald, John, (2012), Robust Tracking for Real-Time Dense RGB-D Mapping with Kintinuous, CSAIL Technical Reports (https://dspace.mit.edu/handle/1721.1/73167).

WHO. Air Quality Guidelines for Europe, 2nd edn, World Health Organization Regional Office for Europe, Copenhagen, Denmark, WHO Regional Publications, European Series, No. 91, 2000, Available: https://apps.who.int/iris/bitstream/handle/10665/107335/E71922.pdf (Accessed : 19 November 2019).

W. Holt, A. Safaeinili, J. J. Plaut, J. W. Head, R. J. Phillips, R. Seu, S. D. Kempf, P. Choudhary, D. A. Young, N. E. Putzig, D. Biccari, Y. Gim, Radar sounding evidence for buried glaciers in the southern mid-latitudes of Mars. Science 322, 1235–1238 (2008). doi:10.1126/science.1164246pmid:19023078

Wilhelm, R., Radtke, K., Mykytczuk, N., Greer, C. and Whyte, L., 2012. Life at the Wedge: the Activity and Diversity of Arctic Ice Wedge Microbial Communities. Astrobiology, 12(4), pp.347-360.